Theoretical Study of CO Migratory Insertion Reactions with Group 10 Metal−Alkyl and −Alkoxide Bonds

Stuart A. Macgregor* and Greg W. Neave

School of Engineering and Physical Sciences, William H. Perkin Building, Heriot-Watt University, Edinburgh, EH14 4AS, U.K.

Received June 18, 2003

The results of density functional calculations on the alternative migratory insertion reactions of CO with the M−OMe and M−Me bonds of group 10 M(Me)(OMe)$(PH_3)_2$ model systems are reported. For all three metals insertion into the M−OMe bond to form methoxycarbonyl products is thermodynamically favored over insertion into the M−Me bond to give acyls. This preference is small when M = Ni ($\Delta\Delta E_R$ = 3 kcal/mol) but increases down the triad and becomes significant for M = Pt ($\Delta\Delta E_R$ = 12 kcal/mol). Both associative five-coordinate and phosphine displacement four-coordinate mechanisms for migratory insertion were considered. For Ni associative mechanisms are more accessible and the lowest energy pathway is for reaction with the Ni−Me bond. With Pd and Pt the five- and four-coordinate pathways are close in energy, and for Pd there is a small kinetic preference for insertion into the Pd−OMe bond. For Pt however there is a clear kinetic preference for reaction with the Pt−OMe bond. During migratory insertion into M−OMe bonds the methoxide ligand rotates in the transition state to allow the participation of an oxygen lone pair in C−O bond formation while maintaining some residual M···OMe interaction. This M···OMe interaction is retained to some extent in the three-coordinate methoxycarbonyl species formed along the four-coordinate pathways. For an isostructural series of reactive species the trend in activation energy is always Ni < Pd ≪ Pt for reaction with the M−Me bond and Ni > Pd < Pt (with Pt > Ni) for reaction with the M−OMe bond. Trends in the computed thermodynamic and kinetic data of the alternative migratory insertions can be understood in terms of metal−ligand homolytic bond strengths. All M−C bonds studied show a marked increase down the group 10 triad, whereas much less variation is seen in the M−OMe bonds, which results in reaction with the M−OMe bonds being generally favored. A key additional driving force, however, is the stronger C−O bond formed in the methoxycarbonyl product compared to the C−C bond of the alternative acyl species.

Introduction

The organometallic chemistry of low-valent transition metal−oxygen bonds has developed rapidly over the last two decades.[1] The isoelectronic relationship between alkoxide and alkyl ligands suggests that they may display similar chemistry. Indeed, low-valent group 10 metal−oxygen bonds have been shown to participate in a number of typical organometallic reactions, including C−O bond forming reductive elimination,[2] β-H elimination,[3] and insertion reactions with unsaturated molecules such as CO[4−13] and alkenes.[14] However, the presence of lone pairs on the oxygen atom and the "hard" character of O-based ligands point to differences in stability and reactivity that may occur for these species relative to carbon-based analogues.

The present work focuses on CO insertion reactions with low-valent group 10 metal−methoxide bonds to form methoxycarbonyl species. Two general mechanisms for this process may be envisaged (Scheme 1). Pathway I requires CO to bind to form an intermediate from which an intramolecular migratory insertion process can occur. Alternatively, in pathway II CO initially displaces

* Corresponding author. E-mail: S.A.Macgregor@hw.ac.uk.

(1) (a) Bryndza, H. E.; Tam, W. *Chem. Rev.* **1988**, *88*, 1163. (b) Fryzuk, M. D.; Montgomery, C. D. *Coord. Chem. Rev.* **1989**, *95*, 1. (c) Fulton, J. R.; Holland, A. W.; Fox, D. J.; Bergman, R. G. *Acc. Chem. Res.* **2002**, *35*, 44.

(2) (a) Muci, A. R.; Buchwald, S. L. *Top. Curr. Chem.* **2002**, *219*, 131. (b) Williams, B. S.; Goldberg, K. I. *J. Am. Chem. Soc.* **2001**, *123*, 2576. (c) Mann, G.; Incarvito, C.; Rheingold, A. L.; Hartwig, J. F. *J. Am. Chem. Soc.* **1999**, *121*, 3224. (d) Han, R.; Hillhouse, G. L. *J. Am. Chem. Soc.* **1997**, *119*, 8135.

(3) (a) Zhao, J.; Hesslink, H.; Hartwig, J. F. *J. Am. Chem. Soc.* **2001**, *123*, 7220. (b) Blum, O.; Milstein, D. *J. Organomet. Chem.* **2000**, *594*, 479. (c) Blum, O.; Milstein, D. *J. Am. Chem. Soc.* **1995**, *117*, 4582. (c) Bryndza, H. E.; Calabrese, J. C.; Marsi, M.; Roe, C. D.; Tam, W.; Bercaw, J. E. *J. Am. Chem. Soc.* **1986**, *108*, 4805. (d) Macgregor, S. A.; Sweeney, B. *New J. Chem.* **2000**, *24*, 855.

(4) Bryndza, H. E. *Organometallics* **1985**, *4*, 1686.

(5) (a) Kim, Y.-J.; Osakada, K.; Takenaka, A.; Yamamoto, A. *J. Am. Chem. Soc.* **1990**, *112*, 1096. (b) Kim, Y.-J.; Osakada, K.; Sugita, K.; Yamamoto, T.; Yamamoto, A. *Organometallics* **1988**, *7*, 2182. (c) Komiya, S.; Akai, Y.; Tanaka, K.; Yamamoto, T.; Yamamoto, A. *Organometallics* **1985**, *4*, 1130.

(6) Tóth, I.; Elsevier, C. J. *J. Chem. Soc., Chem. Commun.* **1993**, 529.

(7) Smith, G. D.; Hanson, B. E.; Merola, J. S.; Waller, F. J. *Organometallics* **1993**, *12*, 568.

(8) Kapteijn, G. M.; Dervisi, A.; Verhoef, M. J.; van den Broek, M. A. F. H.; Grove, D. M.; van Koten, G. *J. Organomet. Chem.* **1996**, *517*, 123.

(9) Dockter, D. W.; Fanwick, P. E.; Kubiak, C. P. *J. Am. Chem. Soc.* **1996**, *118*, 4846.

(10) (a) Bennett, M. A.; Rokicki, A. *Organometallics* **1985**, *4*, 180. (b) Bennett, M. A.; Yoshida, T. *J. Am. Chem. Soc.* **1978**, *100*, 1750.

10.1021/om030459c CCC: $25.00
Publication on Web 09/30/2003

Scheme 1

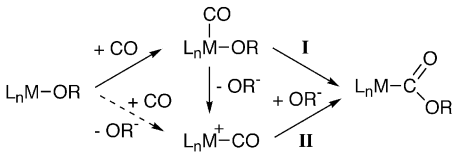

the anionic OR^- ligand, which then acts as a nucleophile at the bound cationic carbonyl. Evidence for both types of processes has been presented,[4,12,15] although in many cases the intimate details of the apparent insertion process have not been elucidated. The reactivity of group 10 M(R)(OR′)L_2 complexes (L = phosphines, L_2 = P- or N-based chelate ligands) has been extensively studied and provides the opportunity for the direct comparison of M−C and M−O bonds. With Pt(Me)(OMe)(dppe) (dppe = 1,2-bis(diphenylphosphino)ethane) CO inserts exclusively into the Pt−OMe bond,[4] and other reports have highlighted the enhanced reactivity of Pt−O over Pt−C bonds.[10,11] The situation is less clear with related Pd and Ni complexes, as rapid reductive elimination of an ester usually occurs after initial CO insertion, although in several instances spectroscopic characterization of Pd−alkoxycarbonyl intermediates suggests a greater reactivity for Pd−alkoxide bonds[5b,6,8] compared to Pd−alkyl bonds. Migratory insertion of CO into a Pd−OMe bond has also been put forward as a possible initiation step for CO/ethene copolymerization.[16] The best characterized CO migratory reactions with Ni−O bonds involve complexes featuring aryloxide ligands such as Ni(Me)(O-*p*-C_6H_4CN)L_2 (L = PEt_3; L_2 = 2,2′-bipyridyl), for which spectroscopic evidence for the formation of an acyl intermediate was found, indicating a greater reactivity of the Ni−Me bond in this case.[5c] In general, M−alkoxides appear more reactive than M−aryloxides,[5a,8] although the reasons for this remain unclear. A key role for the O-based lone pairs in facilitating the migratory insertion process has been identified, although the relative strengths of the M−O and M−C bonds may also be important.[9]

Many theoretical studies of CO migratory insertion reactions with group 10 M−alkyl bonds have been reported, and this process has been characterized in terms of migration of the alkyl species onto the neighboring carbonyl ligand.[17] In studies where the effect of the group 10 metal center has been directly compared, it is found that migratory insertion is more favorable both kinetically and thermodynamically for Pd compared to Pt,[18] while one previous study comparing Ni and Pd found a preference for the Ni system.[19] The issue

Scheme 2

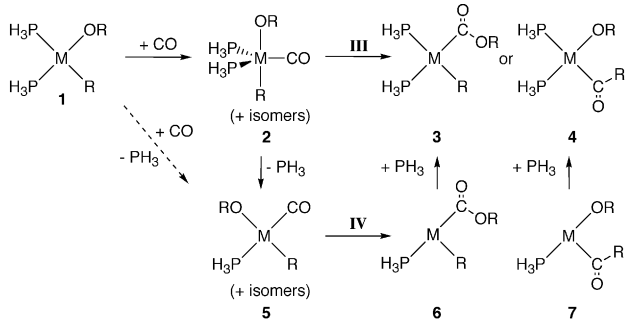

of competing four- versus five-coordinate pathways has also been addressed with the latter being more accessible in Ni systems.[20] In addition, several studies have highlighted the existence of "ligand-assisted" pathways whereby a neutral ligand is displaced by CO but remains loosely bound in the transition state. The displaced ligand either may be monodendate[21] or may be one arm of a chelating ligand.[22] In contrast to the extensive literature on CO migratory insertion with group 10 metal−alkyl bonds, we are unaware of any previous theoretical studies on the equivalent reaction with group 10 metal−alkoxide bonds or indeed any type of metal−oxygen bond.

In the present paper we use density functional calculations to investigate the CO migratory insertion with group 10 M(Me)(OMe)$(PH_3)_2$ model systems. Only intramolecular migratory insertion processes will be considered, from either five-coordinate species of the type M(Me)(OMe)(CO)$(PH_3)_2$ (pathway III, Scheme 2) or four-coordinate M(Me)(OMe)(CO)(PH_3) species (pathway IV). Our aims are to define the general features of CO migratory insertion with low-valent M−OMe bonds, to compare the migratory aptitudes of the methyl and methoxide ligands, and to assess the effect of the central metal on these migratory insertion processes.

Computational Details

Calculations used the Amsterdam Density Functional program ADF1999.[23] A triple-ζ-STO basis set was employed for metal atoms, while all other atoms were described by a double-ζ plus polarization STO basis set. The frozen core approximation was employed for the 1s electrons of C and O, up to and including the 2p electrons of P and Ni, the 4d electrons of Pd, and the 4f electrons of Pt. All geometry optimizations used the procedure developed by Versluis and

(11) Michelin, R. A.; Napoli, M.; Ros, R. *J. Organomet. Chem*. **1979**, *175*, 239.
(12) (a) Stang, P. J.; Zhong, Z. D. *Organometallics* **1992**, *11*, 1026. (b) Huang, T.-M.; You, Y.-J.; Ching-Shuenn, Y.; Tzeng, W.-H.; Chen, J.-T.; Cheng, M.-C.; Wang, Y. *Organometallics* **1991**, *10*, 1020.
(13) Yasuda, H.; Choi, J.-C.; Lee, S.-C.; Sakakura, T. *Organometallics* **2002**, *21*, 1216.
(14) (a) Bennett, M. A.; Jin, H.; Li, S.; Rendina, L. M.; Willis, A. C. *J. Am. Chem. Soc*. **1995**, *117*, 8335. (b) Bryndza, H. E. *Organometallics* **1985**, *4*, 406.
(15) (a) Bernard, K. A.; Atwood, J. D. *Organometallics* **1989**, *8*, 795. (b) Rees, W. M.; Churchill, M. R.; Fettinger, J. C.; Atwood, J. D. *Organometallics* **1985**, *4*, 2179.
(16) Drent, E.; Budzelaar, P. H. M. *Chem. Rev*. **1996**, *96*, 663.
(17) (a) Koga, N.; Morokuma, K. *Chem. Rev*. **1991**, *91*, 823. (b) Cavell, K. J. *Coord. Chem. Rev*. **1996**, *155*, 209. (c) Niu, S.; Hall, M. B. *Chem. Rev*. **2000**, *100*, 353. (d) Dedieu, A. *Chem. Rev*. **2000**, *100*, 543.
(18) (a) Koga, N.; Morokuma, K. *J. Am. Chem. Soc*. **1985**, *107*, 7230. (b) Koga, N.; Morokuma, K. *J. Am. Chem. Soc*. **1986**, *108*, 6136. (c) Kayaki, Y.; Tsukamoto, H.; Kaneko, M.; Shimuzu, I.; Yamamoto, A.; Tachikawa, M.; Nakajima, T. *J. Organomet. Chem*. **2001**, *622*, 199.
(19) Svensson, M.; Matsubara, T.; Morokuma, K. *Organometallics* **1996**, *15*, 5568.
(20) (a) Bernardi, F.; Bottoni, A.; Nicastro, M.; Rossi, I.; Novoa, J.; Prat. X. *Organometallics* **2000**, *19*, 2170. (b) De Angelis, F.; Sgamellotti, A.; Re. N. *Organometallics* **2002**, *21*, 2036.
(21) Markies, B. A.; Wijkens, P.; Dedieu, A.; Boersma, J.; Spek, A. L.; van Koten, G. *Organometallics* **1995**, *14*, 5628.
(22) (a) Groen, J. H.; Zwart, A. d.; Vlaar, M. J. M.; Ernsting, J. M.; van Leewven, P. W. N. W.; Vrieze, K.; Kooijman, H.; Smeets, W. J. J.; Spek, A. L.; Budzelaar, P. H. M.; Xiang, Q.; Thummel, R. P. *Eur. J. Inorg. Chem*. **1998**, 1129. (b) Frankcombe, K. E.; Cavell, K. J.; Yates, B. F.; Knott, R. B. *Organometallics* **1997**, *16*, 3199.
(23) Baerends, E. J.; Ellis, D. E.; Ros, P. *Chem. Phys*. **1973**, *2*, 41. (b) te Velde, G.; Baerends, E. J. *J. Comput. Phys*. **1992**, *99*, 84. (c) Fonseca Guerra, C.; Snijders, J. G.; te Velde, G.; Baerends, E. J. *Theor. Chem. Acc*. **1998**, *99*, 391.

Ziegler[24] and incorporated the gradient corrections due to Becke[25] (exchange) and Perdew[26] (correlation) as well as the quasi-relativistic corrections of Snijders and co-workers.[27] To test functional dependency, we also studied the reactions of CO with Pt(Me)(OMe)$(PH_3)_2$ using the PW91[28] and BLYP[29] functionals but found no significant energy changes occurred. All stationary points were fully optimized with no symmetry constraints, and transition states were characterized using numerical frequency analyses[30] and were shown to have a unique imaginary frequency corresponding to the expected migratory insertion process. All energies quoted in the text are uncorrected for thermal and zero-point energy effects. The nature of the energy minima linked via a given transition state was then confirmed by first distorting the transition state geometry forward and back along the unique imaginary eigenvector and then allowing the structure to relax to either reactant or product in subsequent geometry optimizations. In some cases extra low energy imaginary frequencies were obtained which generally corresponded to PH_3 ligand rotation. On occasion, test calculations on alternative PH_3 orientations failed to remove these, but did indicate that the energy change associated with this movement was negligible. For the five-coordinate M(Me)(OMe)(CO)$(PH_3)_2$ species the various possible isomers were searched for by first assuming a trigonal bypyramidal structure and imposing all possible symmetry constraints. The structures thus obtained were then reoptimized without any symmetry or angle constraints to give the local minima reported in the text. Bond dissociation energies were computed by comparing the energies of the radical species produced by homolytic metal−ligand bond cleavage, fully optimized via spin-unrestricted calculations, against the energy of the full molecule.

Results

Structures of M(Me)(OMe)$(PH_3)_2$ Species. For all three metals the cis isomer of M(Me)(OMe)$(PH_3)_2$ was computed to be more stable than the trans form (by 3.5 kcal/mol for M = Ni and Pd and by 6.7 kcal/mol for M = Pt), and details of the former are shown in Figure 1. Crystallographic studies on group 10 *cis*-M(alkyl)(alkoxide)L_2 species consistently show alkoxide ligands exert a smaller trans influence than alkyl ligands, and this is well reproduced by the calculated M−P bond distances.[3c,31] For M = Pd or Pt the computed M−OMe and M−Me distances are within the range known experimentally, while the computed Ni−OMe distance in *cis*-Ni(Me)(OMe)$(PH_3)_2$ agrees well with that of the only crystallographically characterized organometallic Ni−alkoxide, Cp*Ni(OMe)(PEt_3).[32] In the calculations

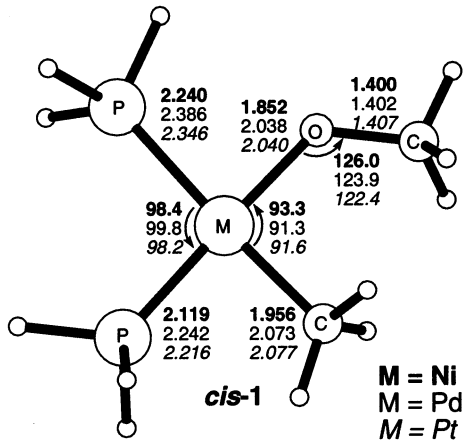

Figure 1. Selected computed geometric parameters (Å, deg) for *cis*-M(Me)(OMe)$(PH_3)_2$, ***cis*-1**. Data for M = Ni in bold, for M = Pd in normal text, and M = Pt in italics.

the methoxide ligand is always found to lie in the metal coordination plane with a O−Me bond length of around 1.40 Å. A short O−C bond is a feature of low-valent transition metal alkoxides, with values in the range 1.258(12)[3c] to 1.38(2) Å[29b] having been determined. Our calculations therefore appear to overestimate the O−Me distance, although the computed values are still shorter than that of free methanol (1.420 Å).[33]

Migratory Insertion of CO via Five-Coordinate Species. M = Ni. Using the method described in the Computational Details three isomers of Ni(Me)(OMe)(CO)$(PH_3)_2$, **2a−c(Ni)**, were located and are shown in Figure 2. The most stable isomer (**2a(Ni)**, $E = -18.4$ kcal/mol) is formed via CO addition to *trans*-Ni(Me)(OMe)$(PH_3)_2$ and exhibits a trigonal bipyramidal structure with both the PH_3 ligands and CO in equatorial positions, reflecting the preference for π-acid ligands for this site in a d^8 ML_5 complex.[34] The OMe ligand is oriented such that the O−C bond is eclipsed with respect to the Ni−CO bond. The remaining two isomers are formed via CO addition to *cis*-Ni(Me)(OMe)$(PH_3)_2$ to give distorted square-pyramidal structures with axial PH_3 ligands and CO trans to either OMe (**2b(Ni)**, $E = -16.8$ kcal/mol) or Me (**2c(Ni)**, $E = -9.7$ kcal/mol).[35] The long axial Ni−P distances in **2b(Ni)** (2.416 Å) and **2c(Ni)** (2.376 Å) suggest that the axial PH_3 ligands are relatively weakly bound, while the greater stability of **2b(Ni)** over **2c(Ni)** presumably results from enhanced stabilizing "pull−push" interactions between trans CO and OMe ligands.[36] This also results in a very short Ni−CO distance in **2b(Ni)** (1.728 Å), although, by contrast, little variation is computed in the Ni−O distances in **2a−c(Ni)**.

The three five-coordinate intermediates **2a−c(Ni)** allow for four possible migratory insertion pathways: from **2a(Ni)** with either the Ni−Me or the Ni−OMe bond (via **2a(Ni)-TS(C)** or **2a(Ni)-TS(O)**, respectively, Figure 2), from **2b** with the Ni−Me bond (**2b(Ni)-TS-**

(24) (a) Versluis, L.; Ziegler, T. *Chem. Phys.* **1988**, *88*, 322. (b) Fan, L.; Ziegler, T. *J. Am. Chem. Soc.* **1992**, *114*, 10890.
(25) Becke, A. D. *Phys. Rev. A* **1988**, *38*, 3098.
(26) Perdew, J. P. *Phys. Rev. B* **1986**, *33*, 8822.
(27) (a) Snijders, J. G.; Baerends, E. J.; Ros, P. *Mol. Phys.* **1979**, *38*, 1909. (b) Ziegler, T.; Tschinke, V.; Baerends, E. J.; Snijders, J. G.; Ravenek, W. *J. Phys. Chem.* **1989**, *93*, 3050. (c) van Lenthe, E.; Baerends, E. J.; Snijders, J. G. *J. Chem. Phys.* **1993**, *99*, 4597.
(28) Perdew, J. P.; Chevary, J. A.; Vosko, S. H.; Jackson, K. A. Pederson, M. R.; Singh, D. J.; Fiolhais, C. *Phys. Rev., B* **1992**, *46*, 6671.
(29) (a) Lee, C.; Yang, W.; Parr, G.. *Phys. Rev., B* **1988**, *37*, 785. (b) Johnson, B. G.; Gill, P. M. W.; Pople, J. A. *J. Chem. Phys.* **1993**, *98*, 5612. (c) Russo, T. V.; Martin, R. L.; Hay, P. J. *J. Chem. Phys.* **1994**, *101*, 7729.
(30) Fan, L. Ziegler, T. *J. Chem. Phys.* **1992**, *96*, 9005. (b) Fan, L.; Ziegler, T. *J. Chem. Phys.* **1992**, *96*, 6937.
(31) (a) Osakada, K.; Kim, Y.-J.; Tanaka, M.; Ishiguro, S.; Yamamoto, A. *Inorg. Chem.* **1991**, *30*, 197. (b) Osakada, K.; Kim, Y.-J.; Yamamoto, A. *J. Organomet. Chem.* **1990**, *382*, 303. (c) Kapteijn, G. M.; Dervisi, A.; Grove, D. M.; Kooijman, H.; Lakin, M. T.; Spek, A. L.; van Koten, G. *J. Am. Chem. Soc.* **1995**, *117*, 10939.
(32) Holland, P. L.; Smith, M. E.; Andersen, R. A.; Bergman, R. G. *J. Am. Chem. Soc.* **1997**, *119*, 12815.

(33) Test calculations run with both larger basis sets (ADF basis sets IV and V on the ligands) and the PW91 and BLYP functionals gave no significant computed geometrical changes. Further calculations showed the orientation of the OMe ligand does not affect the O−Me bond length.
(34) Rossi, A. R.; Hoffmann, R. *Inorg. Chem.* **1975**, *14*, 365.
(35) Reaction profiles showed that the addition of CO to either *cis*- or *trans*-Ni(Me)(OMe)$(PH_3)_2$ occurred with minimal activation barriers.
(36) Caulton, K. J. *New J. Chem.* **1994**, *18*, 25.

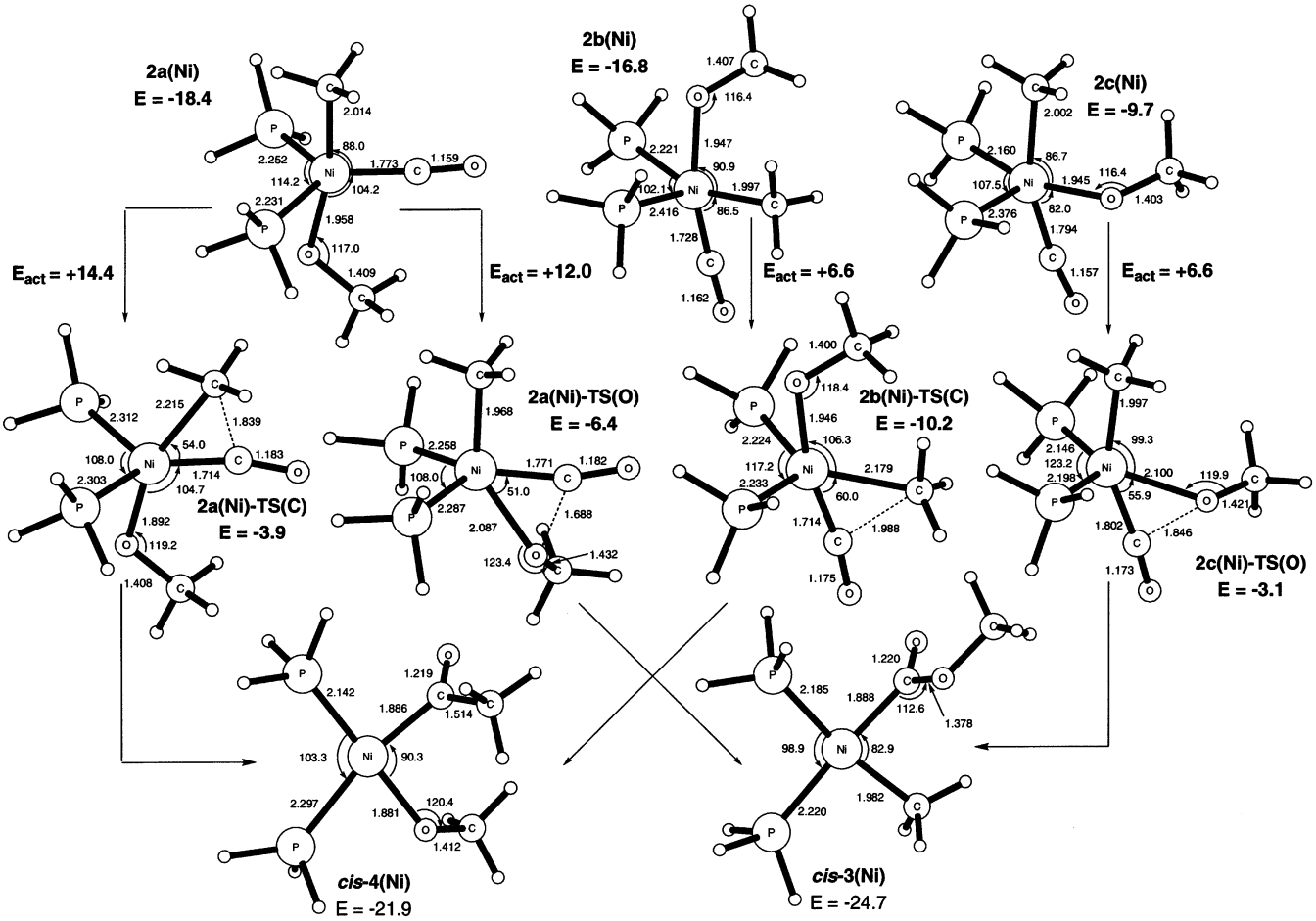

Figure 2. Selected computed geometric parameters (Å, deg) and relative energies (kcal/mol) for the stationary points for the migratory insertion reactions of ***cis*-1(Ni)** with CO via five-coordinate Ni(Me)(OMe)(CO)$(PH_3)_2$, **2(Ni)**. Energies are relative to ***cis*-1(Ni)** + free CO set to zero.

(C)), and from **2c** with the Ni−OMe bond (**2c(Ni)-TS-(O)**). The computed structures of **2a(Ni)-TS(C)** and **2a(Ni)-TS(O)** suggest these reactions correspond to migration of the relevant axial ligand onto the equatorial CO, with lengthening of the bond between Ni and the migrating ligand and a shortening of the bond trans to this. Although **2a(Ni)-TS(C)** retains near C_s symmetry, in **2a(Ni)-TS(O)** the methoxide group has rotated (C_{Me}−O−Ni−C_{CO} = −91.5° compared to 9.0° in **2a(Ni)**), suggesting the participation of an oxygen lone pair in C−O bond formation by donation into the CO π^* orbital. In addition, the Ni−OMe bond in **2a(Ni)** lengthens by only 0.129 Å to form **2a(Ni)-TS(O)**, whereas the Ni−Me bond must lengthen by 0.201 Å to form **2a(Ni)-TS(C)**. These observations suggest that some residual Ni···OMe interaction is maintained in **2a-(Ni)-TS(O)**, while the initial Ni−Me interaction in **2a-(Ni)** is sacrificed to a greater extent in **2a(Ni)-TS(C)** (Scheme 3). Moreover, calculation of the Ni−OMe migratory insertion process under the constraint of C_s symmetry, where such lone pair participation is precluded, resulted in a transition state that was 13.7 kcal/mol higher in energy than the C_1 transition state. Overall, **2a(Ni)-TS(O)** is 2.5 kcal/mol more stable than **2a(Ni)-TS(C)**.

The migratory insertions from square-pyramidal **2b-(Ni)** and **2c(Ni)** proceed with a shortening of the axial Ni−P bonds, and both **2b(Ni)-TS(C)** and **2c(Ni)-TS-**

Scheme 3

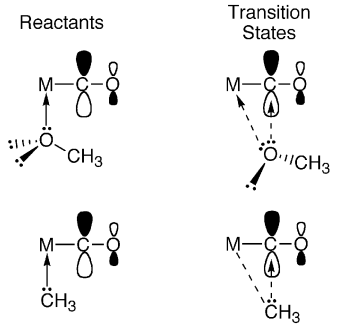

(O) resemble trigonal bipyramidal structures in which the axial CO and equatorial Me or OMe ligands have moved toward each other. Comparing **2b(Ni)-TS(C)** with **2a(Ni)-TS(C)** shows the former to have an earlier structure, in terms of both a longer forming C···C bond and a shorter breaking Ni−Me bond. The activation energy (ΔE_{act}) required to reach **2b(Ni)-TS(C)** from **2b-(Ni)** (+6.6 kcal/mol) is lower than that required to reach **2a(Ni)-TS(C)** from **2a(Ni)** (+14.4 kcal/mol), and, overall, **2b(Ni)-TS(C)** is 6.3 kcal/mol more stable than **2a-(Ni)-TS(C)**. In **2c(Ni)-TS(O)** a rotation of the methoxide ligand similar to that seen above for **2a(Ni)-TS(O)** is computed (C_{Me}−O−Ni−C_{CO} = −93.0°). **2c(Ni)-TS(O)** also exhibits an earlier transition state structure and lower activation energy than **2a(Ni)-TS(O)** (ΔE_{act} =

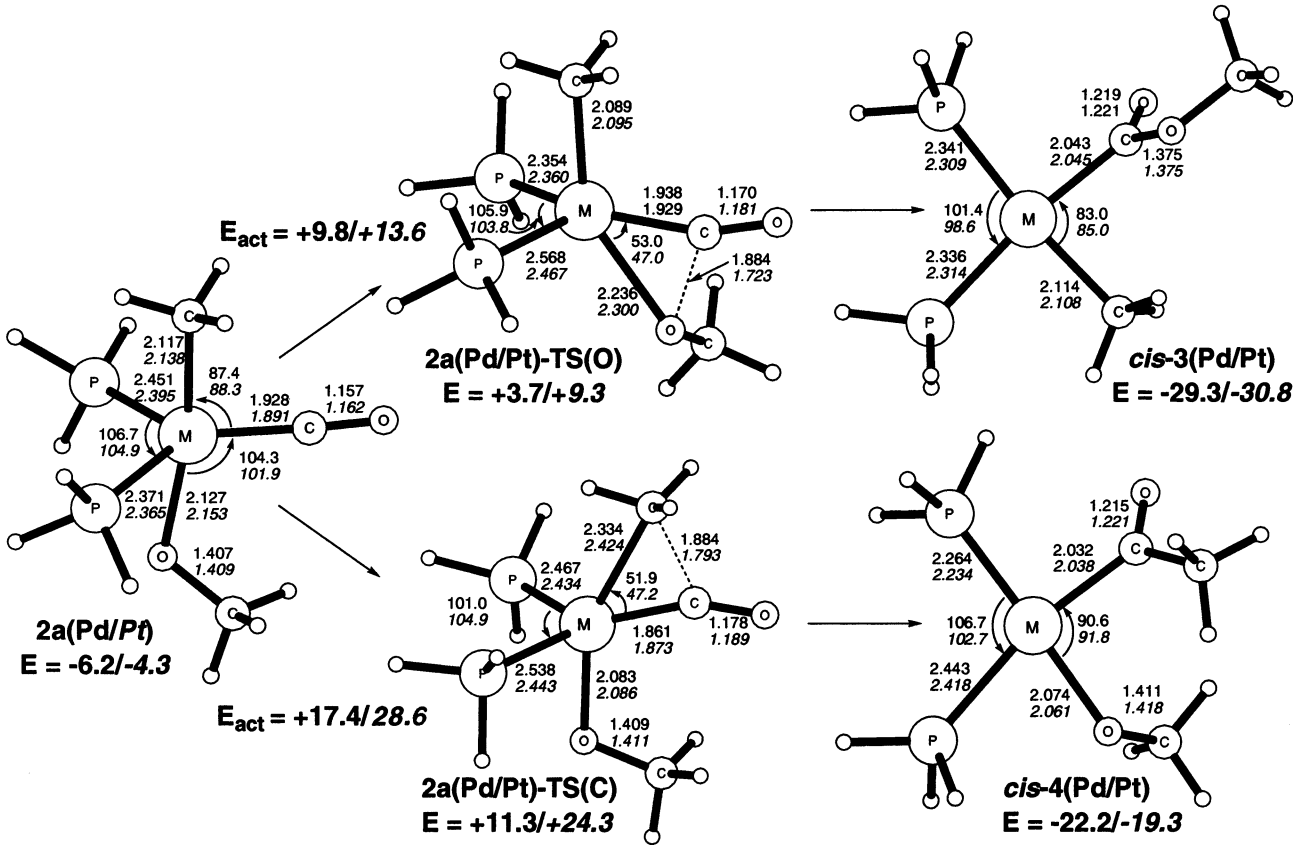

Figure 3. Selected computed geometric parameters (Å, deg) and relative energies (kcal/mol) for stationary points for the migratory insertion reactions of ***cis*-1(Pd/Pt)** with CO via five-coordinate M(Me)(OMe)(CO)$(PH_3)_2$, **2a(Pd/Pt)**. Data for M = Pd are given in normal text, while data for M = Pt are in italics. Energies are relative to ***cis*-1(Pd/Pt)** + free CO set to zero.

+6.6 kcal/mol, cf. +12.0 kcal/mol), although the higher energy of intermediate **2c(Ni)** means that **2c(Ni)-TS(O)** is still 3.3 kcal/mol higher in energy than **2a(Ni)-TS(O)**. Of the four migratory insertion transition states **2b(Ni)-TS(C)** is the most accessible, being 3.8 kcal/mol more stable than **2a(Ni)-TS(O)**. Reaction with the Ni−Me bond is therefore kinetically favored, assuming facile formation of **2b(Ni)**.[37]

The products of migratory insertion are either a methoxycarbonyl species, Ni$(CO_2Me)(Me)(PH_3)_2$, **3(Ni)**, or an acyl species, Ni{C(O)Me}$(OMe)(PH_3)_2$, **4(Ni)**. Characterization of the migratory insertion transition states suggests that the initial products are the trans isomers; however in general the cis isomers were found to be more stable, and these are shown in Figure 2. We have not studied the trans−cis isomerization process. Both cis products exhibit square-planar coordination, with the acyl and methoxycarbonyl moieties lying approximately perpendicular to the coordination plane, as is typical for such species. In general, the computed geometries of the acyl and methoxycarbonyl ligands agree well with experimental values[38] and the very long Ni−P bond trans to the acyl group in ***cis*-4** indicates a high trans influence for this ligand. Formation of the methoxycarbonyl product is slightly more exothermic than the alternative acyl ($\Delta E_R = -24.7$ and −21.9 kcal/mol, respectively). Thus, while migratory insertion into the Ni−Me bond is favored kinetically, there is a small thermodynamic preference for reaction with the Ni−OMe bond.

M = Pd, Pt. In contrast to Ni, for Pd and Pt only one isomer of M(Me)(OMe)(CO)$(PH_3)_2$ could be located, and this exhibited both PH_3 ligands and CO in equatorial positions (**2a(Pd/Pt)**, Figure 3). Attempts to locate other isomers resulted in either isomerization back to **2a** or PH_3 dissociation to give CO-substituted four-coordinate structures (see below). This difference reflects both the greater tendency of Ni to form five-coordinate species and a decreased CO binding energy down the triad (ΔE_{adduct}, see Table 1). The structures of **2a(Pd)** and **2a(Pt)** and their associated transition states for migratory insertion into either the M−OMe bonds (**2a(Pd/Pt)-TS(O)**, E = +3.7/+9.3 kcal/mol) or M−Me bonds (**2a(Pd/Pt)-TS(C)**, E = +11.3/+24.3 kcal/mol) are broadly similar to their Ni counterparts, with the rotation of the methoxide ligand again being evident in **2a(Pd/Pt)-TS(O)**. A greater asymmetry in the M−P bonds is found however, especially when M = Pd. The difference in the M−OMe and M−Me bond elongations from **2a(Pd/Pt)**

(37) **2b(Ni)** can be formed directly via CO addition to *cis*-Ni(Me)(OMe)$(PH_3)_2$ or, in principle, via isomerization of **2a(Ni)**. Attempts to locate such isomerization pathways, however, led instead to phosphine dissociation, and it seems more likely that the **2a/2b(Ni)** interconversion will proceed via CO loss, *cis*/*trans* isomerization of **1(Ni)**, and then readdition of CO to give **2b/2c(Ni)**. Therefore, if *cis*/*trans* isomerization is difficult, starting from the trans isomer of Ni(Me)(OMe)$(PH_3)_2$ would lead to methoxycarbonyl formation via **TS-2a(O)**, but starting from the cis isomer would favor acyl formation via **2b-TS(C)**.

(38) Cambridge Structural Database. (a) Allen, F. H. *Acta Crystallogr.* **2002**, *B58*, 380. (b) Bruno, I. J.; Cole, J. C.; Edgington, P. R.; Kessler, M.; Macrae, C. F.; McCabe, P.; Pearson, J.; Taylor, R. *Acta Crystallogr.* **2002**, *B58*, 389.

Table 1. Energetics (kcal/mol) for CO Migratory Insertion with M(Me)(OMe)$(PH_3)_2$ Species via Five-Coordinate Intermediates[a]

		ΔE_{act}		ΔE_R	
	ΔE_{adduct}	into M−Me	into M−OMe	into M−Me	into M−OMe
2a(Ni)	−18.4	+14.4 (−3.9)	+12.0 (−6.4)	−21.9	−24.7
2a(Pd)	−6.2	+17.4 (+11.3)	+9.8 (+3.7)	−22.2	−29.3
2a(Pt)	−4.3	+28.6 (+24.3)	+13.6 (+9.3)	−19.3	−30.8
2b(Ni)	−16.8	+6.6 (−10.2)		−21.9	
2c(Ni)	−9.7		+6.6 (−3.1)		−24.7

[a] ΔE_{adduct} is the energy of CO addition to ***cis*-1(M)**; ΔE_{act} is the computed activation energy relative to the appropriate isomer of **2(M)**. The relative energy of each transition state is given in parentheses; ΔE_R is the computed overall change in energy upon migratory insertion to form ***cis*-3(M)** or ***cis*-4(M)**, relative to ***cis*-1(M)**.

to reach these transition states is even greater than was noted for **2a(Ni)** above, resulting in an increasing kinetic preference for insertion into the M−OMe bonds ($\Delta\Delta E_{act}$ = 7.6 kcal/mol for M = Pd and 15.0 kcal/mol for M = Pt).

In addition to these transition states derived from isomer **2a(Pd/Pt)**, we were also able to locate the Pd and Pt transition states **2b(Pd/Pt)-TS(C)** and **2c(Pd/Pt)-TS(O)**, which are analogous to the Ni transition states **2b(Ni)-TS(C)** and **2c(Ni)-TS(O)**. The energies of **2c(Pd/Pt-TS(O)** (E = +3.7 and 7.1 kcal/mol for Pd and Pt, respectively) are similar to those of **2a(Pd/Pt)-TS(O)**; however we found these transition states connect to the four-coordinate reactants M(Me)(OMe)(CO)(PH_3), where CO is trans to Me (**5c**, see below) and one PH_3 ligand has dissociated. **2c(Pd/Pt)-TS(C)** therefore correspond to transition states for PH_3-assisted migratory insertion where the overall reaction with M(Me)(OMe)$(PH_3)_2$ would involve initial displacement of PH_3 by CO, with PH_3 then returning to the coordination sphere during the insertion process. The energies of **2b(Pd/Pt)-TS(C)** (+4.3 and +12.1 kcal/mol for Pd and Pt, respectively) make them competitive with the transition states of the M−OMe reactions, especially for Pd. However, **2b(Pd/Pt)-TS(C)** are also PH_3-assisted migratory insertion transition states, connecting to another isomer of M(Me)(OMe)(CO)(PH_3), where CO is now trans to OMe (**5b**, see below). The synchronous recoordination of PH_3 during migratory insertion that is required for these processes would seem unlikely in bulk solution.[39] It is possible, however, that suitable donor solvent molecules could play an analogous role to PH_3 in these transition states. Generally, intramolecular migratory insertion into group 10 M−O bonds has been observed in weakly coordinating solvents in which solvent-assisted mechanisms would be less important. However in donor solvents transition states related to **2b(Pd/Pt)-TS(C)** could be low enough in energy such that insertion into Pd− and Pt−alkyl bonds could be promoted.

The energetics of the CO migratory insertion reaction via five-coordinate intermediates for all three group 10 metals are summarized in Table 1. These show an increasing thermodynamic preference down the triad for the formation of the methoxycarbonyl products over the alternative acyl species. This arises from an increasing exothermicity of insertion into M−OMe bonds coupled with relatively small changes associated with insertion into the M−Me bonds. Activation energies for the reactions of the isostructural **2a(M)** series show a marked increase for insertion into the M−Me bonds down the triad, while much less variation is seen for insertion into the M−OMe bonds, the latter following the trend M = Ni > Pd < Pt. For M = Pd and Pt there is therefore a clear kinetic and thermodynamic preference for migratory insertion into the M−OMe bond when the reaction proceeds via a five-coordinate pathway. For M = Ni this thermodynamic preference remains, although reaction via isomer **2b(Ni)** provides a kinetically favored route for insertion into the Ni−Me bond.

Migratory Insertion of CO via Four-Coordinate Species Three isomers are possible for the PH_3-substituted species M(Me)(OMe)(CO)(PH_3) (**5a**−**c**), and these are shown in Figure 4 for M = Pt along with the stationary points for the four subsequent reaction profiles for CO migratory insertion with that metal.[40] Details of the analogous structures located for M = Ni and Pd are given as Supporting Information. For all three metals the most stable form of M(Me)(OMe)(CO)(PH_3) has CO trans to OMe (**5b**), as this maximizes the "push−pull" interactions between these ligands. For Ni and Pd the least stable isomer features CO trans to Me (isomer **5c**), while for Pt the isomer with CO trans to PH_3 is least stable (isomer **5a**). The geometries of these four-coordinate complexes can be understood in terms of π-interaction and ligand trans influence effects. Thus M−OMe and M−CO bonds are shortest in **5b**, but these species also have the longest M−P bonds, PH_3 being trans to Me. M−OMe bonds are also longest trans to Me in isomer **5a**, in which, unlike **5b** and **5c**, the OMe ligand lies out of the metal coordination plane.

The three different isomers of M(Me)(OMe)(CO)(PH_3) lead to four pathways for CO migratory insertion. Thus, **5a** can react via **5a-TS(C)** or **5a-TS(O)**, **5b** via **5b-TS(C)** and **5c** via **5c-TS(O)**. In general, changes in bond lengths between linked four-coordinate reactants and transition states are equivalent to those described for migratory insertion via five-coordinate species, and for **5a-TS(O)** the rotated OMe group is again seen. In contrast, for **5c-TS(O)** the OMe ligand lies in the coordination plane and exhibits a near-linear {M···O-

(39) These transition states are similar to those located by Markies et al. for the reaction of CO with Pd$(NH_3)_2CH_3)_2$.[21] Cartesian coordinates for **2b(Pd/Pt)-TS(C)** and **2c(Pd/Pt)-TS(O)** are given in the Supporting Information.

(40) Species **5a**, **5b**, and **5c(Ni)** can be formed via PH_3 dissociation from **2a**, **2b**, and **2c(Ni)**, respectively, and reaction profiles for the reverse process, PH_3 addition to **5a**−**c(Ni)**, show them to be virtually barrierless. Similarly **5a(Pd/Pt)** are readily formed via PH_3 dissociation from **2a(Pd/Pt)**. The formation of **5b(Pd/Pt)** and **5c(Pd/Pt)** however requires PH_3/CO substitution reactions from ***cis*-1(Pd/Pt)**. We have not looked at these processes specifically, but they are expected to be relatively low in energy, as this has been found to be the case for the analogous reactions of Pt(Me)(OMe)$(H_2PCH_2CH_2PH_2)$. Macgregor, S. A.; Neave, G. W. Unpublished results.

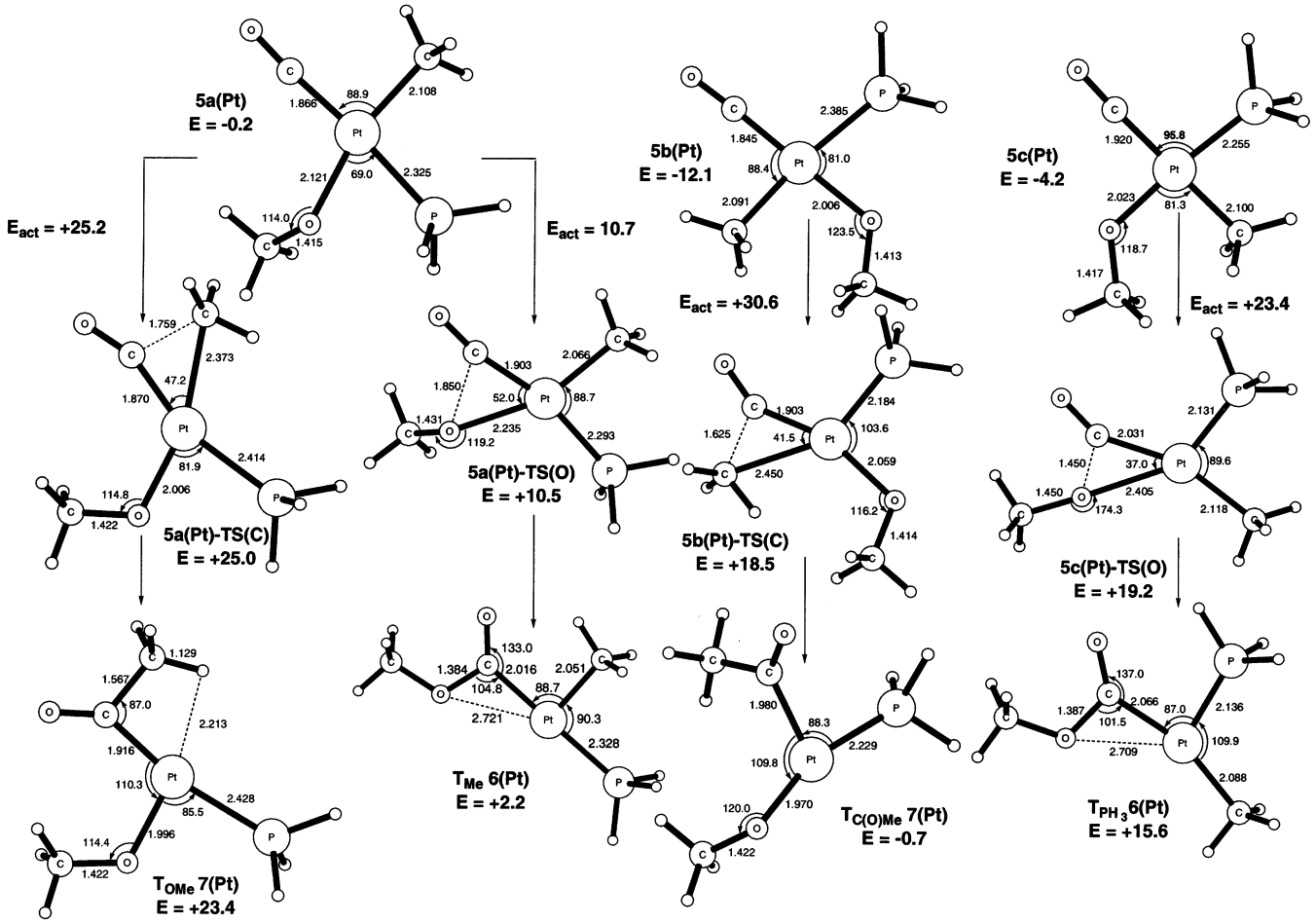

Figure 4. Selected computed geometric parameters (Å, deg) and relative energies (kcal/mol) for stationary points for the migratory insertion reactions of ***cis*-1(Pt)** with CO via four-coordinate M(Me)(OMe)(CO)(PH_3), **5(Pt)**. Energies are relative to ***cis*-1(Pt)** + free CO set to zero.

Me} unit.[41] This is consistent with a very late transition state geometry for these species, which all exhibit product-like C···O distances (<1.5 Å) and near-planar {M−CO_2Me} moieties. In general, for all three metals a given migratory insertion process leads to the same type of three-coordinate intermediate being formed. Thus, insertion into M−OMe bonds leads to the methoxycarbonyl species, M(CO_2Me)(Me)(PH_3), **6**, which exhibits either a T_{Me} (from **5a**) or T_{PH_3} (from **5c**) geometry. The structures of both forms of **6** suggest that a residual M···OMe interaction is retained in these species, with the methoxycarbonyl unit being characterized by small M−C−O and large M−C═O angles, slightly elongated C−O bonds, and relatively short M···OMe contacts.[42] Migratory insertion with M−Me bonds leads to the three-coordinate acyl intermediate, M{C(O)Me}(OMe)(PH_3), **7**. For **5a(Ni)**, this process is coupled to isomerization away from the potential T_{OMe} form to give $T_{C(O)Me}$ **7(Ni)**. The equivalent reactions of **5a(Pd)** and **5a(Pt)** lead to a T_{OMe} structure that is stabilized by an agostic interaction between the metal center and a C−H bond of the acyl−Me group. With **5b** migratory insertion is coupled for all three metals to an isomerization of the potential T_{PH_3} product to give the $T_{C(O)Me}$ form of **7**.

The energetics of these four-coordinate migratory insertion processes are summarized in Table 2. For a given isomer the computed trends in ΔE_{act} are similar to those highlighted above for the five-coordinate reactions. Thus for migratory insertion into the M−Me bonds of intermediate **5a** or **5b** ΔE_{act} follows the trend Ni < Pd ≪ Pt, while with the M−OMe bonds of **5a** or **5c** the trend is Ni > Pd < Pt (with Pt > Ni). Reactions with the M−OMe bonds also entail lower ΔE_{act} from isomer **5a** when OMe is trans to Me rather than from isomer **5c** when OMe is trans to PH_3. This is consistent with the greater trans influence of Me facilitating reaction through a weakening of the metal interaction with the migrating species. Such effects are well established in the CO migratory insertion reactions of PtPh(X)(CO)(PR_3) species (X = Cl, Br, I; PR_3 = PEt_3, PMe_2Ph, $PMePh_2$, PPh_3)[43] and have been noted in previous theoretical studies of CO migratory insertion.[18]

(41) We have been unable to locate a stationary point corresponding to **5c(Ni)-TS(O)**. Instead the energy of the O-bound product, T_{Me} **6(Ni)**, provides a lower limit for the computed activation energy. Linear transit calculations indicate that the potential energy surface around this species is very flat, and this coupled with the "late" nature of the transition states located for the Pd and Pt analogues suggests **5c(Ni)-TS(O)** lies close in energy to T_{Me} **6(Ni)**.

(42) The strength of the M···OMe interaction in **6** was estimated by recalculating the structures of T_{Me} and T_{PH_3} **6** with the M−C−O angles fixed at the "normal" values determined for the equivalent four-coordinate products, ***cis*-3**. This revealed the M···OMe interaction to be strongest in the Ni systems (6.6 kcal/mol in T_{Me} **6(Ni)** and 4.0 kcal/mol in T_{PH_3} **6(Ni)**), consistent with the greatest distortion of the methoxycarbonyl moiety being seen in **6(Ni)**. The equivalent figures for the Pd and Pt analogues are 1.2 kcal/mol (T_{Me} **6(Pd)**), 2.5 kcal/mol (T_{PH_3} **6(Pd)**), 2.4 kcal/mol (T_{Me} **6(Pt)**), and 1.6 kcal/mol (T_{PH_3} **6(Pt)**).

Table 2. Energetics (kcal/mol) for CO Migratory Insertion with M(Me)(OMe)$(PH_3)_2$ Species via Four-Coordinate Intermediates[a]

		ΔE_{act}		ΔE_R	
	ΔE_{sub}	into M−Me	into M−OMe	into M−Me	into M−OMe
5a(Ni)	−8.6	+12.1 (+3.5)	+10.2 (+1.6)	−3.5	+9.9
5a(Pd)	−3.6	+16.2 (+12.6)	+8.0 (+4.4)	+11.4	−2.8
5a(Pt)	−0.2	+25.2 (+25.0)	+10.7 (+10.5)	+23.6	+2.4
5b(Ni)	−15.6	+13.5 (−2.1)		+2.7	
5b(Pd)	−10.0	+15.0 (+5.0)		+2.4	
5b(Pt)	−12.1	+30.6 (+18.5)		+11.4	
5c(Ni)	−7.1		+15.0 (+7.9)		+15.0
5c(Pd)	−2.9		+10.0 (+7.1)		+7.9
5c(Pt)	−4.2		+23.4 (+19.2)		+19.8

[a] ΔE_{sub} is the energy associated with CO substitution relative to ***cis*-1(M)**; ΔE_{act} is the computed activation energy relative to the appropriate isomer of **5(M)**. The relative energy of each transition state is given in parentheses; ΔE_R is the computed change in energy upon migratory insertion to form the various isomers of **6** and **7** relative to the appropriate isomer of **5(M)**. See text for details.

The four-coordinate migratory insertion reactions are completed by PH_3 addition to **6** or **7** to form four-coordinate M$(CO_2Me)(Me)(PH_3)_2$ (**3**) or M{C(O)Me}-$(OMe)(PH_3)_2$ (**4**). This may occur directly to the various forms of **6** and **7** described above, or these three-coordinate species may first undergo isomerization to a more stable form prior to PH_3 addition.[44] To ensure that such processes do not incur a significant activation barrier over and above that for the migratory insertion step, we have studied the PH_3 addition step for T_{Me} and T_{PH_3} **6(Ni)** (which feature the strongest, and so presumably the most difficult to displace, M···OMe interactions[42]) and T_{OMe} **7(Pt)** species. In all cases a reaction profile for the addition of PH_3 led smoothly to the bis-PH_3 product with a minimal activation energy (<1 kcal/mol).

The data in Table 2 show that for Ni the most accessible four-coordinate transition state is **5b(Ni)-TS-(C)**, which is 3.7 kcal/mol more stable than the lowest energy transition state for insertion into the Ni−O bond (**5a(Ni)-TS(O)**), indicating a small kinetic preference for insertion into the Ni−C bond. For Pd and Pt, as was the case via the five-coordinate pathways, insertion into the M−OMe bond becomes favored kinetically, although this preference is very small for Pd (**5a(Pd)-TS(O)** is only 0.6 kcal/mol more stable than **5b(Pd)-TS(C)**) but is more significant for Pt (**5a(Pt)-TS(O)** is 8.0 kcal/mol more stable than **5b(Pt)-TS(C)**).

The lowest energy five- and four-coordinate pathways for migratory insertion into the M−OMe and M−Me bonds are shown in Figure 5 for each metal. For Ni the five-coordinate pathways are clearly more accessible and the lowest energy migratory insertion transition state is **2b(Ni)-TS(C)**. This is consistent with experimental studies on the related migratory insertions of CO with Ni(Me)(O-*p*-$C_6H_4CN)L_2$ species, for which a five-coordinate mechanism has been demonstrated.[5c] For Pd and Pt the four- and five-coordinate pathways are close in energy. For Pd the lowest energy process proceeds through **2a(Pd)-TS(O)**, but both **5a(Pd)-TS(O)** and **5b-(Pd)-TS(C)** are close in energy. Only for Pt is a clear kinetic preference for migratory insertion with the Pt−OMe bond computed, with both **2a(Pt)-TS(O)** and **5a-(Pt)-TS(O)** being significantly more stable than the lowest energy transition states for insertion into the Pt−Me bond.

Discussion

Our results show that ΔE_R for the reaction of CO with group 10 M(Me)$(OMe)(PH_3)_2$ species is always more favorable for migratory insertion into the M−OMe over the M−Me bond and that this preference increases down the triad. A key factor in determining this trend will be the strength of the M−OMe/M−Me bonds broken and the M−CO_2Me/M−{C(O)Me} bonds formed during migratory insertion, and the computed homolytic bond strengths for these various bonds are reported in Table 3. We have previously shown that density functional calculations are capable of reproducing relative homolytic M−X bond strengths in Pt(Me)(X)(dppe) species (where X = various anionic carbon and heteroatom donor ligands).[45]

The data in Table 3 show that for M−Me insertion both the M−Me bonds of ***cis*-1** and the M−{C(O)Me}-bonds in ***cis*-4** increase in strength to a similar degree upon descending the triad, and this is consistent with the approximately constant value of ΔE_R for this reaction. The M−{C(O)Me} bonds are computed to be only slightly stronger than the M−Me bonds, however, and so the overall exothermicity of around −20 kcal/mol must therefore arise from the formation of a new C−C bond, balanced against the reduction in formal bond order of the CO group upon insertion. For insertion into the M−OMe bonds the new M−CO_2Me bond in ***cis*-3** is again found to increase in strength from Ni to Pt. In contrast, the M−OMe bond strengths in ***cis*-1** follow the trend Ni > Pd < Pt, and the difference between the M−OMe and M−CO_2Me bond strengths widens down the triad in favor of the product, consistent with the increasingly more negative value of ΔE_R for insertion into the M−OMe bond. The metal−ligand bond strengths therefore account for the increased thermodynamic preference for insertion with the M−OMe bond; however, they do not on their own explain the full extent of the preference for insertion into the M−OMe bonds.[46]

(43) Anderson, G. K.; Cross, R. J. *Acc. Chem. Res.* **1984**, *17*, 67.

(44) For Ni and Pd the T_{Me} isomer was the most stable form of **6**, while for Pt the $T_{(CO_2Me)}$ isomer is 2 kcal/mol more stable than the T_{Me} form. For **7** the $T_{C(O)Me}$ isomer is the most stable form for all three metals.

(45) Macgregor, S. A.; Neave, G. W.; Smith, C. *Faraday Discuss.* **2003**, 111.

(46) Indeed, taking only the metal−ligand bond strengths into account suggests insertion into the M−Me bond would be slightly favored for M = Ni by 2.7 kcal/mol but that insertion into the M−OMe bonds would be favored by 1.0 and 5.5 kcal/mol for M = Pd and Pt, respectively.

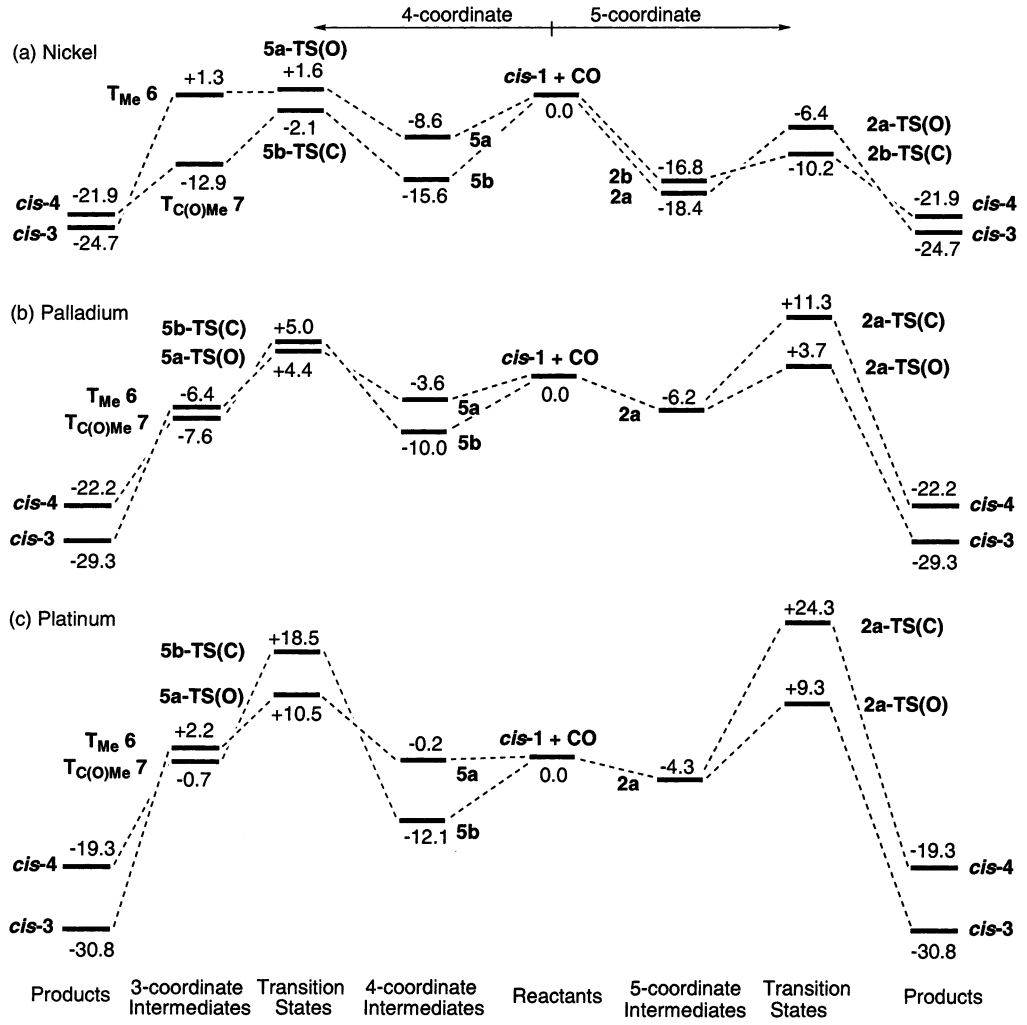

Figure 5. Reaction profiles (kcal/mol) for the lowest energy four- and five-coordinate pathways for CO migratory insertion with M−OMe and M−Me bonds of M(Me)(OMe)$(PH_3)_2$ species.

Table 3. Computed Metal−Ligand Homolytic Bond Dissociation Energies (kcal/mol) in *cis*-M(Me)(OMe)$(PH_3)_2$ (1), M(Me)(OMe)(CO)$(PH_3)_2$ (2a), *cis*-M(Me)$(CO_2Me)(PH_3)_2$ (*cis*-3), *cis*-M{C(O)Me}$(OMe)(PH_3)_2$ (*cis*-4), and the Isomers of M(Me)(OMe)(CO)(PH_3) (5)

	metal−ligand bond	Ni	Pd	Pt
***cis*-1**	M−OMe	60.5	58.9	66.8
	M−Me	40.7	49.7	62.5
2a	M−OMe	49.4	47.2	52.7
	M−Me	41.0	43.9	53.9
***cis*-3**	M−CO_2Me	60.2	63.3	72.8
***cis*-4**	M−{C(O)Me}	43.7	53.1	63.0
5a	M−OMe	57.0	53.6	58.9
	M−Me	34.7	49.8	58.7
5b	M−Me	41.8	49.9	62.4
5c	M−OMe	53.5	53.0	62.0

For this the nature of the new C−O and C−C bonds formed upon insertion must also be considered. Using the C(O)−O bond in methyl acetate (bond dissociation energy = 99 kcal/mol[47]) and the C−C bond in acetone (bond dissociation energy = 80 kcal/mol[47]) as models for these new organic bonds in ***cis*-3** and **-4**, respectively, suggests the former will be significantly stronger and that this factor is at least as important as the metal−ligand bond strengths in determining the preference for migratory insertion into the M−OMe bonds.

We find that the pattern of ΔE_{act} also correlates well with the strength of the bond between the metal and the migrating ligand. For a given reactive intermediate, be it four- or five-coordinate, the same trend in ΔE_{act} is always found, namely, Ni < Pd < Pt for migratory insertion with the M−Me bond and Ni > Pd < Pt (with Pt > Ni) for migratory insertion with the M−OMe bond. These are precisely the trends computed for the M−Me and M−OMe bond dissociation energies computed for ***cis*-1** above, and these trends are retained in the five-coordinate intermediates **2a** and the isomers of the four-coordinate intermediates **5** from which migratory insertion actually takes place (see Table 3).

As with the thermodynamics of the overall migratory insertion process, the absolute kinetic preference for reaction with a M−OMe bond over a M−Me bond cannot be accounted for solely on the basis of relative metal−ligand bond strengths. For example, although migratory insertion with Pt−OMe bonds is preferred kinetically, the Pt−Me and Pt−OMe bonds in **1**, **2**, and **5** are of similar strengths. Other factors must therefore be important here, including the lone pair participation effect in transition states involving a migrating methoxide. A qualitative assessment of this effect can be

(47) *CRC Handbook of Chemistry and Physics*, Weast, R. C., Ed.; CRC Press Inc.: Boca Raton, 1981.

obtained from the calculations on **2a(Ni)**, where the true Ni−OMe transition state located in C_1 symmetry is 13.7 kcal/mol lower in energy than the alternative located when C_s symmetry is imposed. This C_s transition state, for which lone pair participation is ruled out, is 11 kcal/mol above the alternative Ni−Me transition state, and these relative energies in fact better reflect the Ni−ligand bond strengths in **Ni(2a)**, where the Ni−OMe bond is significantly stronger. Finally, as with the products, the relative strengths of the partially formed C···O and C···C bonds in the transition states would also presumably tend to favor the M−OMe migratory insertion processes.

Conclusions

We have presented the results of density functional calculations on competitive CO migratory insertion with the M−Me and M−OMe bonds of group 10 M(Me)(OMe)$(PH_3)_2$ model systems. Our calculations show that there is always a thermodynamic preference for insertion into the M−OMe bond, which is relatively small for Ni ($\Delta\Delta E_R = 3$ kcal/mol) but increases down the triad and becomes significant for Pt ($\Delta\Delta E_R = 12$ kcal/mol). For Ni five-coordinate mechanisms are more accessible kinetically and the lowest energy pathway is for insertion into the Ni−Me bond. For Pd and Pt the four- and five-coordinate pathways are close in energy, and for Pd a small kinetic preference for insertion into the Pd−OMe bond is computed. For Pt the preference for migratory insertion into the M−OMe bond becomes much more significant. The characterization of ligand-assisted transition states for Pd and Pt suggests that donor solvents could promote insertion into Pd− and Pt−Me bonds. For a given isomer the trends in ΔE_{act} are Ni < Pd ≪ Pt for insertion into the M−Me bond and Ni > Pd < Pt (with Pt > Ni) for insertion into the M−OMe bond. Both these trends in ΔE_{act} and that for the thermodynamics of the overall reaction can be understood in terms of the computed M−Me and M−OMe homolytic bond strengths. An important additional factor driving the insertion into the M−OMe bond is the greater strength of the new C−O bond formed in the methoxycarbonyl products compared to the C−C bond formed in the alternative acyl species. This factor could also be important in favoring the M−OMe transition states, which are also stabilized by participation of the methoxide lone pair in C−O bond formation.

Overall our results agree well with the reactivity trends seen experimentally for group 10 M−alkoxide and M−alkyl bonds. Thus the preference for a methoxycarbonyl product with Pt(Me)(OMe)(dppe) is likely to have both kinetic and thermodynamic origins. For Pd the thermodynamic and kinetic preferences for alkoxycarbonyl formation are retained, albeit reduced, while for Ni the lowest energy pathways are for acyl formation, although the methoxycarbonyl is marginally the more stable product. This is consistent with acyl formation upon the reaction of CO with Ni(Me)(O-*p*-$C_6H_4CN)L_2$, although in this case the presence of an aryloxy bond has significant implications for migratory insertion into the Ni−O bond.[48] A detailed study comparing the reactivity of Ni(Me)(O-*p*-C_6H_4CN)(bpy) and Pt(Me)(OMe)(dppe) will form the topic of a subsequent publication.

Acknowledgment. We thank the EPSRC and Heriot-Watt University for support.

Supporting Information Available: Tables of Cartesian coordinates and energies for all stationary points and unique imaginary eigenvalues for all transition states. This material is available free of charge via the Internet at http://pubs.acs.org.

OM030459C

(48) Initial calculations indicate that CO migratory insertion with Ni−OPh bonds is significantly less favorable than the same reaction with Ni−OMe bonds. Neave, G. W. Work in progress.